A novel approach to quantitative spectroscopy of atoms in a magnetic field and applications based on an atomic vapor cell with $L=\lambda$

A. Sargsyan,[1] G. Hakhumyan,[1] A. Papoyan,[1,a)] D. Sarkisyan,[1] A. Atvars,[2] and M. Auzinsh[2]
[1]*Institute for Physical Research, NAS of Armenia, Ashtarak 0203, Armenia*
[2]*Department of Physics, University of Latvia, 19 Rainis Blvd., Riga LV-1586, Latvia*

(Received 26 April 2008; accepted 24 June 2008; published online 17 July 2008)

We describe the so-called λ-Zeeman method to investigate individual hyperfine transitions between Zeeman sublevels of atoms in an external magnetic field of 0.1 mT–0.25 T. Atoms are confined in a nanocell with thickness $L=\lambda$, where λ is the resonant wavelength (794 or 780 nm for D_1 or D_2 line, respectively, of Rb). Narrow resonances in the transmission spectrum of the nanocell are split into several components in a magnetic field; their frequency positions and transition probabilities depend on the B field. Possible applications are described, such as magnetometers with nanometric spatial resolution and tunable atomic frequency references. © *2008 American Institute of Physics*. [DOI: 10.1063/1.2960346]

It is well known that energy levels of atoms placed in an external magnetic field undergo frequency shifts and changes in their transition probabilities. These effects were studied for hyperfine (hf) components of atomic optical transitions (hereafter "hf transitions") in the transmission spectra obtained with an ordinary centimeter-size cell containing Rb and Cs vapor in Ref. 1. However, because of Doppler broadening (hundreds of megahertz), it was possible to partially separate different hf transitions only for $B>0.15$ T. Note that even for these large B values, the lines of ^{87}Rb and ^{85}Rb are strongly overlapped, and pure isotopes have to be used to avoid complicated spectra. In order to eliminate the Doppler broadening, the well-known saturation absorption (SA) technique was implemented to study the Rb hf transitions.[2] However, in this case the complexity of the Zeeman spectra in a magnetic field arises primarily from the presence of strong crossover (CO) resonances, which are also split into many components. That is why, as is mentioned in Ref. 2, the SA technique is applicable only for $B<5$ mT. The CO resonances can be eliminated with selective reflection spectroscopy,[3] but to correctly determine the hf transition position, the spectra must undergo further nontrivial processing. Another method based on the fluorescence spectrum emitted from a nanocell at thickness $L=\lambda/2$ was presented in Ref. 4. However, in this case the sub-Doppler spectral linewidth is relatively large (~100 MHz); also the laser power has to be relatively large to detect a weak fluorescence signal. Coherent population trapping (CPT) allows one to study the behavior of hf transitions in a magnetic field with very high accuracy (several kilohertz),[5] however the experimental realization is complicated. Moreover, measuring hf level shifts of several gigahertz for $B\sim0.1$ T using CPT is not realistic.

We present a method based on narrow (close to natural linewidth) velocity selective optical pumping/saturation (VSOP) resonance peaks of reduced absorption located at the atomic transitions. As was recently shown in Ref. 6, the ratio L/λ is a significant parameter for VSOP resonance formation. The VSOP peaks appear at laser intensity ~1 mW/cm^2 in the transmission spectrum of the nanocell with atomic vapor column of thickness $L=\lambda$, where λ is the resonant wavelength of the laser radiation (794 or 780 nm for Rb D_1 or D_2 line, respectively). At $B>0$, the VSOP resonance is split into several Zeeman components, the number of which depends on the quantum numbers F of the lower and upper levels. The amplitudes of these peaks and their frequency positions depend unambiguously on the B value. This so-called λ-Zeeman method (LZM) allows one to study not only the frequency shift of any individual hf optical transition, but also the modification in transition probability in the region of 0.1 mT–0.25 T (LZM is expected to be valid up to several tesla). Possible applications of a nanocell for diagnostics and mapping of large magnetic gradients and for making widely tunable compact frequency references are addressed too.

Experimental realization of LZM is simple enough (see Fig. 1). The circularly polarized beam of an extended cavity diode laser ($\lambda=794$ nm, $P_L\sim5$ mW, $\gamma_L<1$ MHz) resonant with the ^{87}Rb D_1 transition frequency, after passing through a Faraday isolator, was focused ($\varnothing=0.5$ mm) onto a Rb nanocell with a vapor column of thickness $L=\lambda$ at an angle close to normal. The design of a nanocell is presented in Ref. 6. The source temperature of the atoms of the nanocell was 110 °C, corresponding to a vapor density $N\sim10^{13}$ cm^{-3}, but the windows were maintained at a temperature that was 20 °C higher. Part of the laser radiation was diverted to a centimeter-size Rb cell to obtain a $B=0$ SA spectrum, which served as frequency reference. The nanocell transmission and SA spectra were detected by photodetectors and recorded by

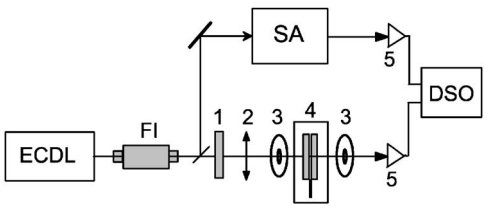

FIG. 1. Experimental setup. FI: Faraday isolator, 1: λ/4 plate, 2: lens ($F=35$ cm), 3: ring magnets, 4: nanocell and the oven, 5: photodetectors, and DSO: digital storage oscilloscope.

a)Author to whom correspondence should be addressed. Electronic mail: papoyan@ipr.sci.am.

 © 2008 American Institute of Physics
Downloaded 18 Jul 2008 to 136.152.208.5. Redistribution subject to AIP license or copyright; see http://apl.aip.org/apl/copyright.jsp

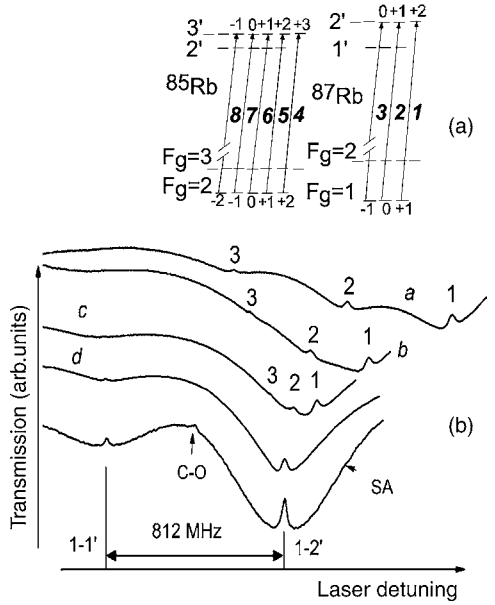

FIG. 2. (a) ^{87}Rb, ^{85}Rb D_1 line atomic transitions, and σ^+ excitation; (b) $F_g=1\rightarrow F_e=1,2$ transmission spectra for $B=$(a) 59 mT, (b) 31 mT, (c) 11.5 mT, and (d) 0; lower curve is SA spectrum. For (d) the value of the peak absorption is ~3% (97% transmission), and the VSOP reduction of peak absorption is ~0.4%.

a digital storage oscilloscope. Small longitudinal magnetic fields ($B<25$ mT) were applied to the nanocell by a system of Helmholtz coils (not shown in Fig. 1). The B-field strength was measured by a calibrated Hall gauge. Among the advantages of LZM is the possibility to apply much stronger magnetic fields using widely available strong permanent ring magnets (PRMs). In spite of the strong inhomogeneity of the B field (in our case it can reach 15 mT/mm), the variation of B inside the atomic vapor column is a few microtesla, i.e., by several orders less than the applied B value because of the small thickness of the nanocell (794 nm).

The allowed transitions between magnetic sublevels of hf states for the ^{87}Rb D_1 line in the case of σ^+ (left circular) polarized excitation are depicted in Fig. 2(a) (LZM also works well for σ^- excitation). Figure 2(b) shows the nanocell transmission spectra for the $F_g=1\rightarrow F_e=1,2$ transitions at different values of B [the labels denote corresponding transitions shown in Fig. 2(a)]. As shown, all the individual Zeeman transitions are clearly detected. The two transitions $F_g=1\rightarrow F_e=1$ [not shown in Fig. 2(a)] are detectable for $B<12$ mT, while at higher B their probabilities are strongly reduced (this is also confirmed theoretically[4]). Note that the absence of CO resonances in transmission spectra is an important advantage of the nanocell.[6]

Transmission spectra for larger B values are presented in Fig. 3 (also for Zeeman transitions of the ^{85}Rb D_1 line). The strong magnetic field was produced by two ∅ 30 mm PRMs, with ∅ 3 mm holes to allow radiation to pass, placed on opposite sides of the nanocell oven and separated by a distance that was varied between 35 and 50 mm (see Fig. 1). To control the magnetic field value, one of the magnets was mounted on a micrometric translation stage for longitudinal displacement. In particular, the B-field difference of curves (a) and (b) is obtained by a PRM displacement of 0.67 mm, corresponding to a rate of 15 mT/mm. The frequency difference between the VSOP peaks numbered 4 [curves (a) and

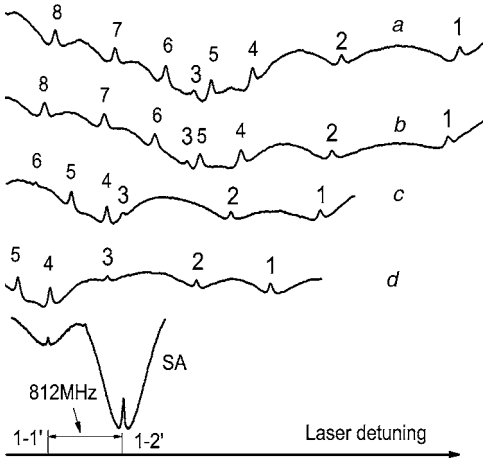

FIG. 3. Transmission spectra for $B=$(a) 0.24 T, (b) 0.23 T, (c) 0.154 T, and (d) 0.117 T; lower curve is SA spectrum.

(b)] for this case is 100 MHz. By a 20 μm displacement of the PRM, it is easy to detect ~3 MHz frequency shift of peak 4. The advantage of a submicron-size magnetic field probe can be fully exploited for the case of a larger B-field gradient as well as after further optimization of the method (reduction in laser intensity, implementation of frequency modulation, lock-in detection, etc.). An important advantage of LZM is that the amplitude of VSOP peaks is linearly proportional to the corresponding Zeeman transition probability, which offers the possibility to quantitatively study the modification of individual Zeeman transition probabilities in a magnetic field. Thus, in weak magnetic fields ($B\approx 0$), the probabilities of transitions labeled 1, 2, and 3 compose the ratio 6:3:1, which varies rapidly as B increases. Figure 4(a) presents the amplitude ratio $A(1)/A(3)$ (curve 1) and $A(1)/A(2)$ (curve 2) as a function of B (hereafter the dots and solid lines denote experiment and theory, respectively). Figure 4(b) shows the frequency difference $\Delta(1,3)$ and $\Delta(1,2)$ between transitions labeled 1 and 3 (curve 1) and 1 and 2 (curve 2) versus B. Obviously, by measuring $\Delta(1,3)$ and $\Delta(1,2)$, it is possible to determine the strength of the magnetic field, even in the absence of reference spectra.

We also implemented LZM to study transitions $F_g=1\rightarrow F_e=0,1,2,3$ of the ^{87}Rb D_2 line ($\lambda=780$ nm; all the other experimental parameters and conditions are the same). The

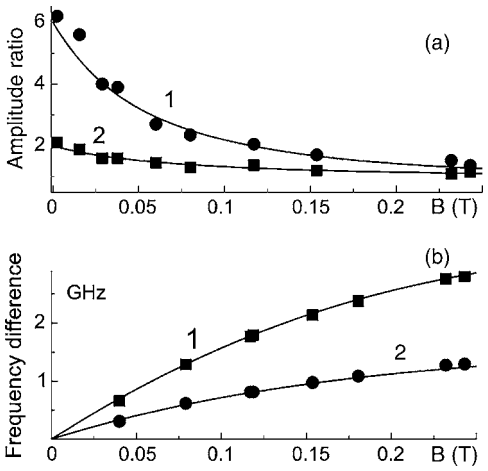

FIG. 4. (a) (1) ratio $A(1)/A(3)$ and (2) ratio $A(1)/A(2)$ vs B. (b) (1) $\Delta(1,3)$ and (2) $\Delta(1,2)$ vs B.

Downloaded 18 Jul 2008 to 136.152.208.5. Redistribution subject to AIP license or copyright; see http://apl.aip.org/apl/copyright.jsp

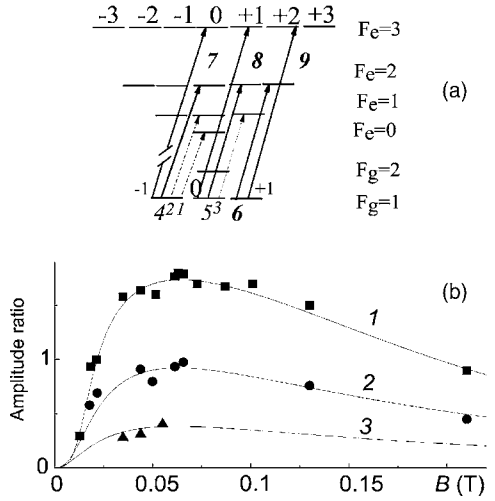

FIG. 5. (a) ^{87}Rb D_2 line atomic transitions and σ^+ excitation. (b) (1) ratio $A(7)/A(6)$, (2) ratio $A(8)/A(6)$, and (3) ratio $A(9)/A(6)$ vs B.

possible Zeeman transitions for σ^+ polarized excitation are depicted in Fig. 5(a). Particularly, it was revealed that for $B>10$ mT, also the ^{87}Rb D_2, $F_g=1\rightarrow F_e=3$ "forbidden" transitions (labeled 7–9) appear in the spectrum, for which new selection rules with respect to the quantum number F apply. Moreover, for 20 mT$<B<$0.2 T the probability of transition 7 exceeds that of transition 6, the strongest transition at $B=0$. Figure 5(b) gives the B-field dependence of amplitude (transition probability) ratio $A(7)/A(6)$, $A(8)/A(6)$, and $A(9)/A(6)$ (curves 1, 2, and 3, respectively). Both in Figs. 4(a) and 5(b), there is good agreement between experiment and theory. The nanocell transmission spectrum for these transitions at $B=0.21$ T is presented in Fig. 6. The two arrows show the positions of the ^{85}Rb $F_g=2\rightarrow F_e=4$ Zeeman transitions (theory[4] well predicts that their probabilities have to be small). The upper insets show the B-field dependence of $\Delta(7,6)$ and $\Delta(8,7)$. We note that transition 7 is strongly shifted (by 5.6 GHz) from the $B=0$ position of the $F_g=1\rightarrow F_e=2$ transition. The latter allows development of a frequency reference based on a nanocell and PRMs, widely tunable over a range of several gigahertz by simple displacement of the magnet. LZM can be successfully implemented also for studies of the D_1 and D_2 lines of Na, K, Cs, and other atoms.

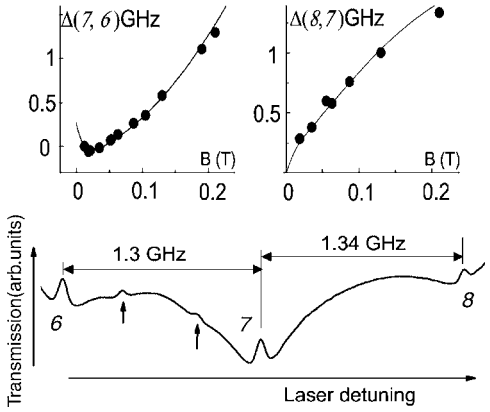

FIG. 6. Transmission spectrum, $B=0.21$ T. Upper insets: $\Delta(7,6)$ (left) and $\Delta(8,7)$ (right) vs B.

This work is partially supported by INTAS S-C Grant No. 06-1000017-9001 and by SCOPES Grant No. IB7320-110684/1. We acknowledge support from the ERAF Grant No. VPD1/ERAF/CFLA/05/APK/2.5.1./000035/018, and A. A. acknowledges support from the ESF project.

[1]P. Tremblay, A. Nichaud, M. Levesque, S. Treriault, M. Breton, J. Beaubien, and N. Cyr, Phys. Rev. A **42**, 2766 (1990).
[2]M. U. Momeen, G. Rangarajan, and P. C. Deshmukh, J. Phys. B **40**, 3163 (2007), and references therein.
[3]N. Papageorgiou, A. Wies, V. Sautenkov, D. Bloch, and M. Ducloy, Appl. Phys. B: Lasers Opt. **59**, 123 (1994).
[4]D. Sarkisyan, A. Papoyan, T. Varzhapetyan, J. Alnis, K. Blush, and M. Auzinsh, J. Opt. A, Pure Appl. Opt. **6**, S142 (2004); D. Sarkisyan, A. Papoyan, T. Varzhapetyan, K. Blush, and M. Auzinsh, J. Opt. Soc. Am. B **22**, 88 (2005). The relative transition probability and magnetic sublevel energy simulation in the magnetic field are based on the eigenvalue and eigenvector dependence from the magnetic field calculation of the Hamilton matrix for the full hfs manifold.
[5]R. Wynands and A. Nagel, Appl. Phys. B: Lasers Opt. **68**, 1 (1999).
[6]D. Sarkisyan, T. Varzhapetyan, A. Sarkisyan, Yu. Malakyan, A. Papoyan, A. Lezama, D. Bloch, and M. Ducloy, Phys. Rev. A **69**, 065802 (2004); C. Andreeva, S. Cartaleva, L. Petrov, S. M. Saltiel, D. Sarkisyan, T. Varzhapetyan, D. Bloch, and M. Ducloy, *ibid.* **76**, 013837 (2007), and references therein; A. Sargsyan, D. Sarkisyan, A. Papoyan, Y. Pashayan-Leroy, P. Moroshkin, A. Weis, A. Khanbekyan, E. Mariotti, and L. Moi, Laser Phys. **18**, 749 (2008).

Downloaded 18 Jul 2008 to 136.152.208.5. Redistribution subject to AIP license or copyright; see http://apl.aip.org/apl/copyright.jsp